scientific reports



OPEN

Pharmacokinetics and the effectiveness of pyrogen-free bioabsorbable wet adhesives

Risa Oshima¹, Kumiko Yoshihara^{2,3⊠}, Ko Nakanishi⁴, Tsukasa Akasaka⁴, Shinji Shimoji¹, Teppei Nakamura⁵, Takumi Okihara⁶, Mariko Nakamura⁷, Akihiro Matsukawa³, Ikkei Tamada⁸, Bart Van Meerbeek⁹, Tsutomu Sugaya¹ & Yasuhiro Yoshida^{4⊠}

Bioabsorbable materials are essential for advanced therapies, including surgical sealing, cell therapy, and drug delivery. Natural bioabsorbable materials, including collagen and hyaluronic acid, have better biocompatibility than synthetic bioabsorbable polymers; however, they are mainly derived from animals, presenting infection risks. Non-animal origin polymers have a lower molecular weight than those of animal origins. Their viscosity increases with increase in molecular weight, making endotoxin removal difficult. Here, using the phosphoryl chloride disposal method, we present a strategy for synthesizing pyrogen-free bioabsorbable adhesives with controlled molecular weight. Phosphopullulan, a polysaccharide derivative, had less than detectable endotoxin levels and controllable average molecular weight of approximately 300,000 to over 1,400,000. Furthermore, it is important to ensure the safety as well as efficacy of bio-implantable materials. We have evaluated the biosafety of polysaccharide derivatives we are developing, and have examined their cell phagocytosis and pharmacokinetics in vitro and in vivo, and have confirmed that they are safe. We have also evaluated their adhesion to wet tissue adhesions and confirmed that they leak less than existing materials.

Keywords Phosphopullulan, Polysaccharide, ADME, Animal study, Endodontic sealer

Collagen, hyaluronic acid, polyglycolic acid, and polylactic acid are widely used in the medical field as bioabsorbable materials. Polyglycolic and polylactic acids, which are synthetic bioabsorbable polymers, cause inflammation because their degradation products are acidic¹. Natural bioabsorbable materials, such as collagen and hyaluronic acid, have better biocompatibility than synthetic bioabsorbable polymers². However, current injectable collagen and hyaluronic acid are mainly derived from animals, thus presenting a risk of infection by unknown viruses and biomolecules. Non-animal-derived collagen and hyaluronic acid have smaller molecular weights than those of animal origin³, limiting their applications. Even if a technology to increase their molecular weights is developed in the future, removing endotoxins would be difficult owing to their higher viscosity^{4,5}. The use of animal-derived materials may become limited in the future to reduce their environmental impact⁶. Furthermore, most surgical sealants representing anti-adhesion materials are used for soft tissues and few for hard tissues because current bioabsorbable materials do not adhere to biological hard tissues^{7,8}. Damage to the teeth and bones directly leads to the loss of essential vital functions, such as eating and moving, respectively⁹. Owing to the growing elderly population worldwide, the need for biological hard tissue reconstruction and regeneration may increase in the near future¹⁰. To enable these therapies, it is essential to develop bioabsorbable adhesives that are nontoxic, tightly bind to wet hard tissues, and work well within highly dynamic environments

¹Department of Periodontology, Faculty of Dental Medicine, Hokkaido University, Sapporo, Japan. ²Health and Medical Research Institute, National Institute of Advanced Industrial Science and Technology (AIST), Takamatsu, Japan. ³Department of Pathology and Experimental Medicine, Graduate School of Medicine, Dentistry and Pharmaceutical Sciences, Okayama University, Okayama, Japan. ⁴Department of Biomaterials and Bioengineering, Faculty of Dental Medicine, Hokkaido University, Sapporo, Japan. ⁵Department of Applied Veterinary Science, Faculty of Veterinary Medicine, Hokkaido University, Sapporo, Japan. ⁶Division of Applied Chemistry, Graduate School of Natural Science and Technology, Okayama University, Okayama, Japan. ⁷Department of Clinical Psychology, School of Clinical Psychology, Kyushu University of Medical and Science, Nobeoka, Japan. ⁸Department of Plastic and Reconstructive Surgery, Tokyo Metropolitan Children's Medical Center, Tokyo, Japan. ⁹BIOMAT, Department of Oral Health Sciences, & UZ Leuven, Dentistry, KU Leuven, Kapucijnenvoer 7, 3000 Leuven, Belgium. [™]email: kumiko.yoshihara@aist.go.jp; yasuhiro@den.hokudai.ac.jp

inside the body. However, despite noteworthy research findings on bone¹¹ and teeth¹², no progress has been made in developing materials that can be effectively used in therapeutic techniques in medicine and dentistry.

To design a highly effective biomaterial with excellent adhesion to moist hard tissues, we synthesized a crosslinked phosphopolymer for wet adhesion using a divalent phosphate group, which has the best binding capacity to hard tissues among functional groups¹³. The polysaccharide pullulan, which is highly water soluble, was selected as the backbone (Fig. 1a). Controlling the molecular weight of polymers is important as it significantly affects their physical properties such as adhesion, viscosity and wettability. We further investigated the synthesis of phosphopulluran and found that phosphopulluran could be synthesised by controlling the molecular weight of the polymer while removing endotoxin (Fig. 1b,c). By selecting phosphopullulan of appropriate molecular weight, it can be made into liquid, powder, gel, sheet or other forms according to the purpose (Fig. 1d).

It is necessary to evaluate the behavior of this phosphorylated pullulan in the body before it can be used in the body. In this study, the in vitro and in vivo behaviour of phosphorylated pullulan in vivo and in vitro using fluorescent labelling and in vivo using ¹⁴C phosphopullulan was elucidated. Furthermore, the efficacy of phosphopullulan as a bone replacement material was evaluated in animal experiments. The sealing properties of phosphopullulan with hard tissue were also investigated by adding phoshopullulan to MTA cement.

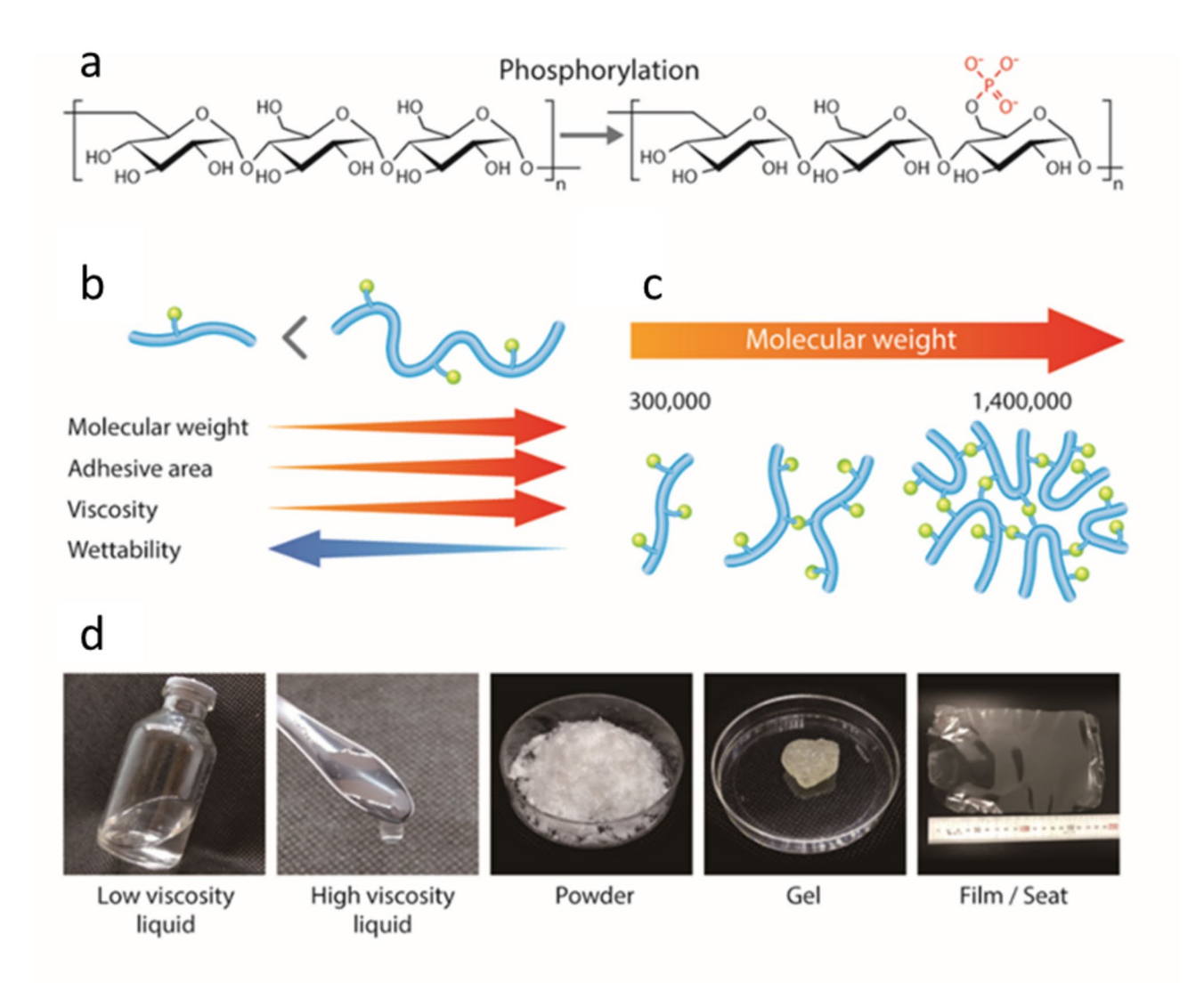


Fig. 1. Key design concepts of pyrogen-free bioabsorbable polymer phosphopullulan. (a) Molecular structure of highly water-soluble polysaccharide pullulan and phosphopullulan. (b) A schematic diagram illustrating the relationship between molecular weight and adhesive area, viscosity, and wettability. As the molecular weight increases, both the adhesive area and viscosity increase, whereas wettability decreases. (c) A schematic diagram illustrating the molecular weight of phosphopullulan and its cross-linking by phosphate groups. An increase in cross-linking with phosphate groups results in a higher molecular weight. (d) Applications of phosphopullulan. By adjusting its molecular weight and processing method, it can be fabricated into various forms, including low-molecular-weight liquids, high-molecular-weight viscous liquids, powders, gels, and films.

Results Synthesis PPL

We attempted three different methods to synthesize "partially cross-linked phosphopullulan": (1) dissolving pullulan in an aqueous phosphoric acid solution and heating at 170 °C for 5 h, (2) subjecting a solid mixture of pullulan and phosphate compounds to microwave irradiation, and (3) dissolving pullulan in aqueous sodium hydroxide solution and treating it with phosphoryl chloride. In method (1), approximately 4% of the OH groups of pullulan were replaced with divalent phosphate groups. Compared to the heating method, method (2) introduced more phosphate groups into pullulan; however, controlling the phosphorylation rate was difficult. The average molecular weight of phosphopullulan obtained using methods (1) and (2) was 20,000–200,000 and 30,000–100,000, respectively. Controlling the average molecular weight of phosphopullulan, which is lower than 320,000, was difficult in both methods. This finding indicates that divalent phosphate groups can be introduced, and very few crosslinks are introduced in methods (1) and (2). Comparably, method (3) provided phosphopullulan with a stable phosphorylation rate. A maximum of 9.6% of the OH groups in pullulan were substituted with divalent phosphate groups. The molecular weight of phosphopullulan can be controlled by cross-linking the molecules through some phosphate groups, leading to the formation of diesters (Fig. 1c). We successfully produced large quantities of phosphopullulan with a controllable average molecular weight of approximately 300,000 to over 1,400,000.

FTIR

FTIR spectra of pullulan and phosphopullulan in wide range of wavenumber $500-4000 \text{ cm}^{-1}$ (Fig. 2a). For the phosphorylated sample, the analysis revealed the appearance of new peaks at 1231 and 921 cm⁻¹, characteristic of P = O and P-OH bond stretching, respectively ¹⁴ (Fig. 2b-d).

NMR

The 1 H NMR spectra of pullulan (PL) and phosphopullulan (PPL) are shown (Fig. 2d). Signal present at 4.7 ppm was caused by residual HDO in the D $_2$ O solvent. Signals around 4.9 and 5.4 ppm correspond to anomeric protons internal to the polymer chain. Pullulan was characterized by three envelope peaks resonating between 3.3 and 4.0 ppm. In the phosphopullulan chain, the peak profile was broadened because the methylene groups bound to the phosphate groups were randomly distributed. This resulted in the shoulder peak from 3.9 to 4.1 ppm 15 .

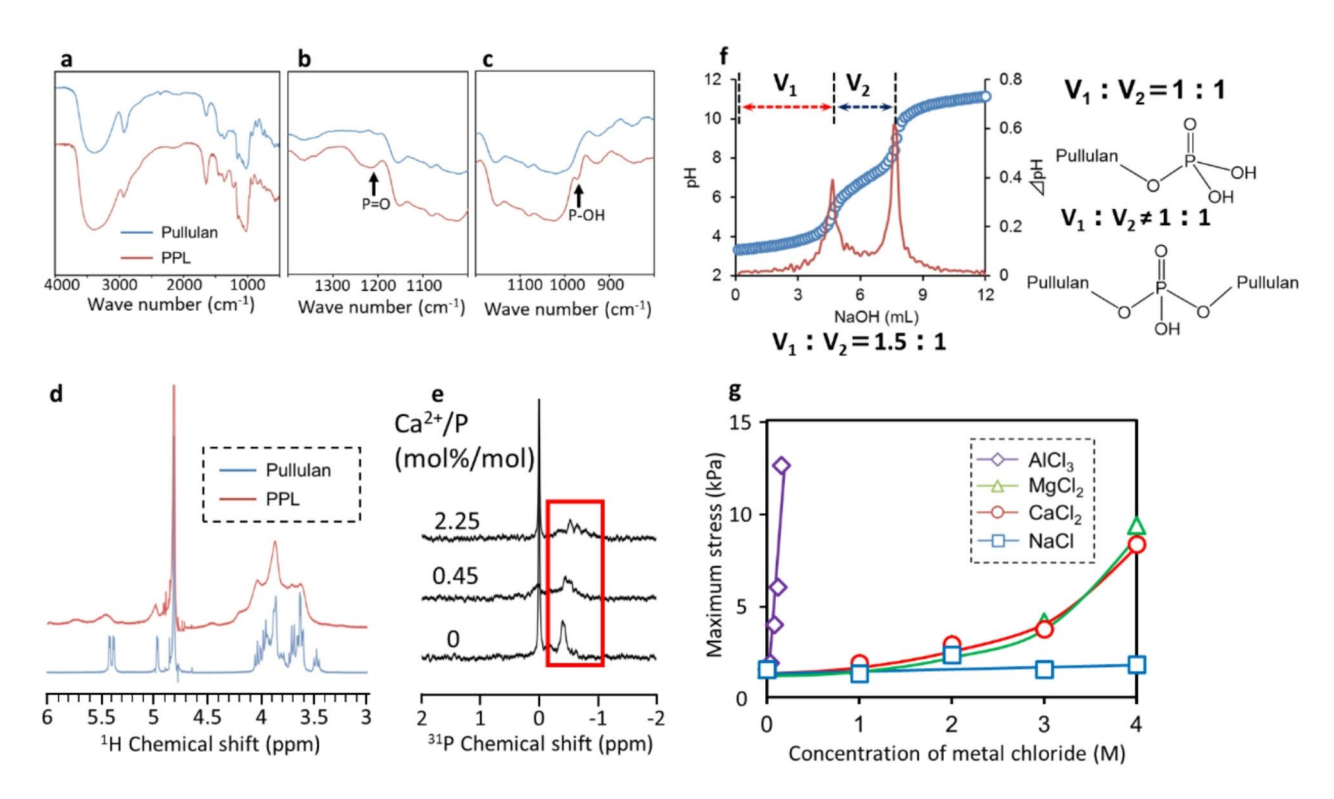


Fig. 2. (**a**–**c**) FTIR spectra of pullulan and phosphopullulan. (**a**) FTIR spectra in wide range of wavenumber 500–4000 cm⁻¹. (**b**) FTIR spectra in narrow range of wave number 1000-1400 cm⁻¹. (**c**) FTIR spectra in narrow range of wave number 800-1200 cm⁻¹. (**d**) 1H NMR spectra of pullulan and phosphorylated pullulan. (**e**) ³¹P NMR was measured by mixing calcium ions and phosphorus in PPL at molar ratios of 0.45:1 and 2.25:1. (**f**) The titration curve of phosphopullulan. The titration curve shows the composition rate of the orthophosphate and crosslinked phosphate groups in phosphopullulan. G. Relationship between maximum intensity and addition of different concentrations of metal ions.

The 31 P NMR spectra of phosphorylated pullulan and phosphorylated with 0.45:1 and 2.25:1 Ca2+:P. The peaks were shifted (Fig. 2e).

Titration curve

The peaks of this differential curve corresponded to the equivalent points of the first and second ionization, respectively (Fig. 2f). The second ionization point did not exactly correspond to twice the first ionization point. This result shows that most of the phosphate groups are orthophosphate, some of which being crosslinked with another pullulan chain¹⁶.

Reaction with metal ion

In the case of NaCl solution, a monovalent metal salt, the stress remained unchanged even with increasing concentration. In contrast, for divalent $MgCl_2$ and $CaCl_2$ solutions, as well as trivalent $AlCl_3$ solution, the adhesive strength increased with increasing concentration (Fig. 2g). In particular, the $AlCl_3$ solution showed a more rapid change in maximum stress than the other aqueous solutions.

POLARIC-labeled PPL

Confocal laser scanning microscopy revealed that phosphopullulan (red) persisted in the cytoplasm 2 h after phagocytosis by macrophages, decreased by 12 h, and had almost disappeared by 24 h (Fig. 3a,b). Phosphorylated pullulan uptake into osteoclasts gradually decreased after phagocytosis and disappeared within 48 h (Fig. 3c). Peritoneal exudate cell neutrophils (green) showed almost no phosphopullulan (red) (Fig. 3d). Phosphorylated pullulan (red) was observed in the cytoplasm of macrophages (green). These results suggest that phosphopullulan is phagocytosed and subsequently digested by macrophages.

IVIS imaging of Alexa flora labeled PPL

Fluorescently labeled phosphorylated pullulan was implanted subcutaneously in mice and in vivo process changes were observed from outside the body (Fig. 4a). It can be seen that the phosphorylated pullulan decreased over time and disappeared after 5 days of absorption (Fig. 4b). The amount injected into the muscle of mice showed the same tendency as that in the subcutaneous region, although the disappearance was faster due to the smaller amount (Fig. 4c).

Animal study of Phosphopullulan gel

In situ tissue regeneration of phosphopullulan gels in rat subcutis after 2 weeks and 4 weeks (Fig. 5 a). Osteocompatibility of phosphopullulan gel implanted in bone defects of rabbits after 4 and 9 weeks (Fig. 5b).

Phosphopullulan is planned to be utilized in various clinical applications, including cranial sutures for craniosynostosis treatment, cleft alveolus in surgical procedures involving cancellous bone grafting, and the lumbar spine for the treatment of compression fractures.

Determination of excretion rate in urine, feces, and exhaled air and percentage of residual in the body using ¹⁴C phosphorylated pullulan

After a single intraperitoneal administration of ¹⁴C phosphorylated pullulan to male rats at a dose of 5 mg/0.5 mL/body, 46.1% of the dose was excreted in urine by 24 h post-dose, 46.8% by 72 h post-dose and 47.5% by 168 h post-dose. In feces, 1.6% of the dose was excreted by 24 h post-dose, 7.5% by 72 h post-dose, and 12.6% by 168 h post-dose. In exhaled air, 1.6% of the dose was excreted by 24 h post-dose, 3.6% by 72 h post-dose, and 5.4% by 168 h post-dose.

The total excretion rate in urine, feces, and exhaled breath up to 168 h post-dose was 65.4% of the administered dose. In addition, 32.2% of the administered dose was found in the body at 168 h post-dose (Fig. 6).

Sealing ability of phosphopullulan (PPL)-containing MTA sealer

The leakage from the root canal sealer is very troublesome, requiring another root canal treatment. The addition of 10% Phosphopullulan to MTA (PPL-containing MTA sealer) was investigated to improve sealing performance while maintaining the existing superior function of the sealer. In order to examine leakage from different sealers. Cross section observation of typical dye leakage after root canal treatment with different endodontic sealers: PPL-containing MTA sealer, resin-based sealer (AH Plus), MTA-containing resin-based sealer (Fillapex), and Zinc oxide non-eugenol sealer (Canals N). Dye leakage (%) of different endodontic sealers with different dentin treatments (paper-point, dry, and wet treatments denoted by a black circle, triangle, and square, respectively). Leakage test revealed that MTA cement with 10% phosphopullulan bonded to dried, paper point dried, and wet dentin surfaces and completely prevented interfacial dye infiltration (p < 0.01) (Fig. 7a). MTA containing resin based sealer and resin based sealer revealed relatively lower leakage when they bonded to dried dentin surface (Fig. 7b). However, leakage was increased when they bonded to wet dentin (Fig. 7c). The zinc oxide non-eugenol sealer exhibited high variability in results across all groups (Fig. 7d).

Calcium release of different endodontic sealers

This graph illustrates the cumulative calcium elution from four different endodontic sealers (Fig. 7e). The resinbased sealer and zinc oxide non-eugenol sealer did not exhibit calcium release. In contrast, the PPA-containing MTA sealer and the MTA-containing resin-based sealer released calcium. The PPA-containing MTA sealer exhibited higher calcium release than the MTA-containing resin-based sealer."

a Synthesis of POLARIC labeled PPL Phosphopullulan Esterification by dehydration condensation agents H₃CO DMT-MM **POLARIC** Phosphopullulan negative 2 h 3 h 24 h 48 h 36 h FITC-Gr-1 F4/80

Fig. 3. Phagocytosis assay of POLARIC-labeled phosphopullulan using Confocal laser scanning microscopy. (a) Synthesis of POLARIC-labeled phosphopullulan. (b) POLARIC-labeled phosphopullulan (red) was observed around the nuclei of RAW 264.7 cells (murine leukemia macrophages), which were stained with DAPI (blue). (c) POLARIC-labeled phosphopullulan (red) was observed around the nuclei of osteoclasts, which were stained with DAPI (blue). (d, e) Phagocytosis of POLARIC-labeled phosphopullulan (red) in intraperitoneal cells analyzed by immunofluorescence staining. (d) Neutrophils were stained with FITC-Gr-1 (green), a neutrophil marker, and DAPI (blue) for nuclei. Phosphopullulan (red) was rarely detected in neutrophils. (e) Macrophages were stained with FITC-F4/80 (green), a macrophage marker, and DAPI (blue) for nuclei. Phosphopullulan (red) was observed within the cytoplasm of macrophages.

a Synthesis of Alexa Fluor 750 labeled PPL

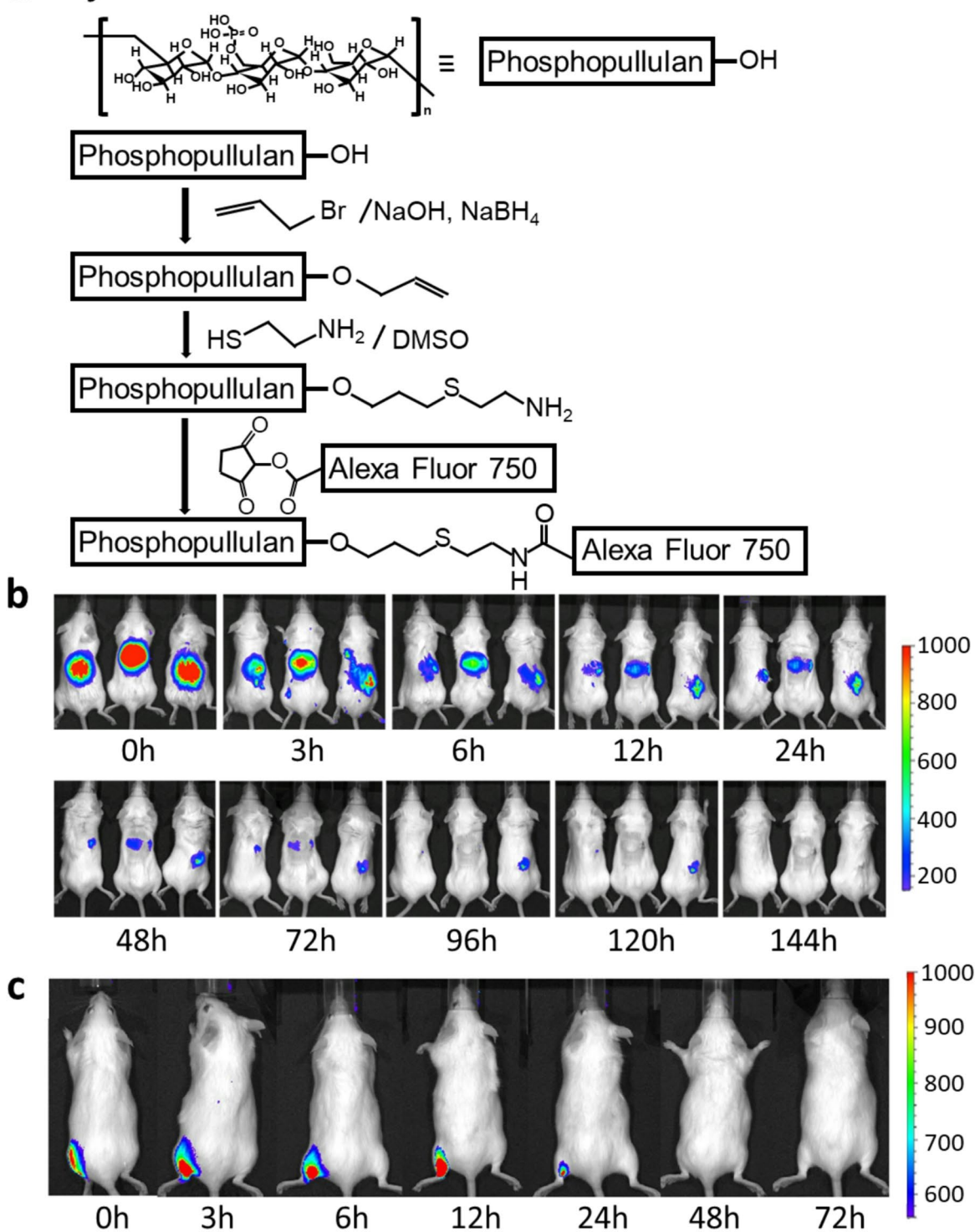


Fig. 4. IVIS imaging of mice at different times after injection with Alexa Fluor 750 labeled PPL. (a) Synthesis of Alexa Fluor 750-labeled phosphopullulan (b) Alexa Fluor 750 labeled PPL was injected intraperitoneally in mice (c) Alexa Fluor 750 labeled PPL was injected submuscularly into the leg of mice.

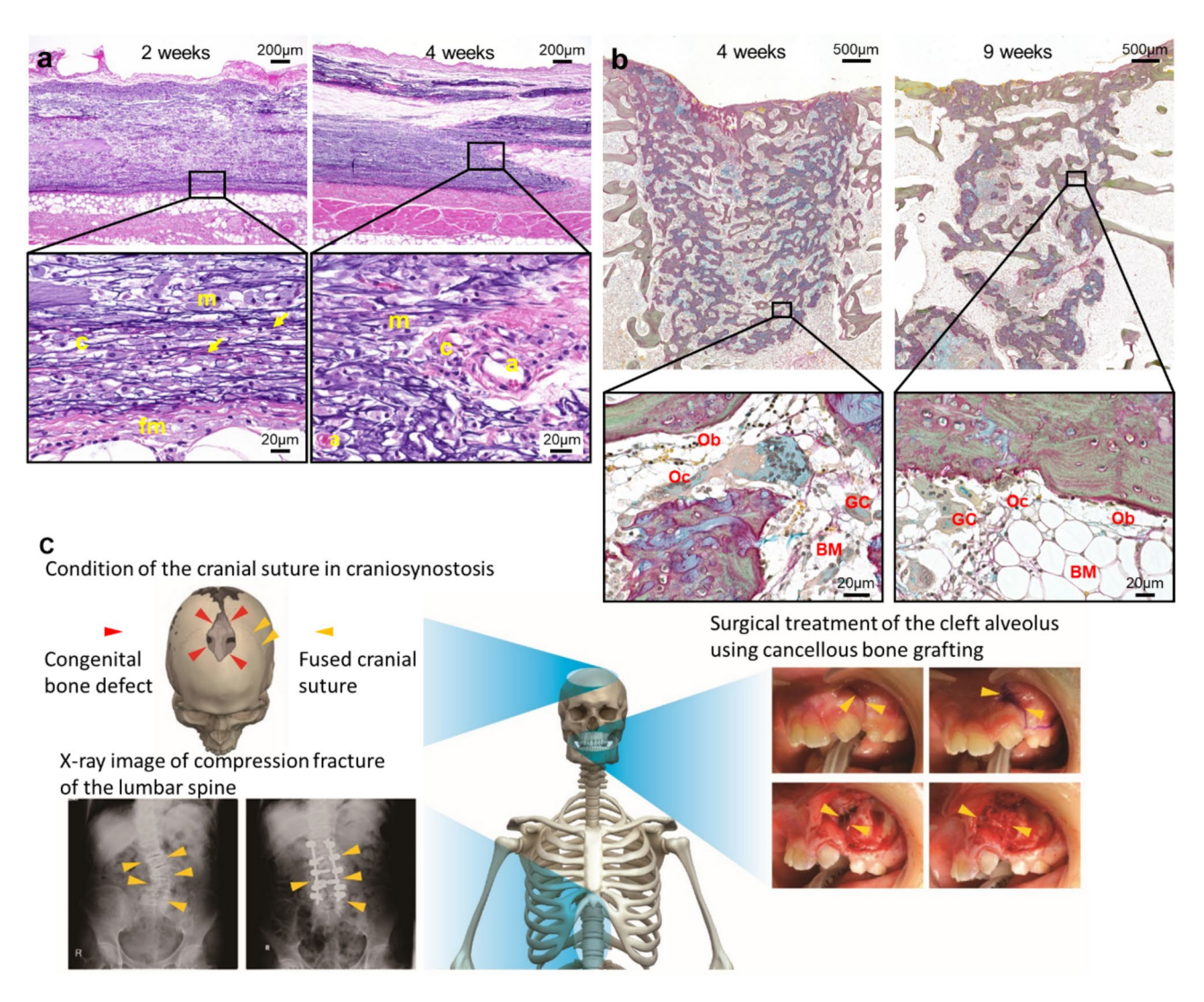


Fig. 5. Applications of phosphopullulan. In situ tissue regeneration of phosphopullulan gels in (a) rat subcutis after 2 weeks and 4 weeks. a: blood vessels; c: connective tissues; fm: fibrous membrane; m: macrophages. Osteocompatibility of phosphopullulan gel implanted in bone defects of rabbits after 4 and 9 weeks (JFRL stain). BM: bone marrow, Ob: osteoblast, Oc: osteoclast, GC: foreign-body giant cell. Examples of sites where pullulan phosphate is used include the cranial sutures in craniosynostosis treatment, cleft alveolus during surgical treatment using cancellous bone grafting, and lumbar spine during treatment of compression fractures.

Apatite precipitation on different endodontic sealer surfaces in simulated body fluids

SEM observation revealed apatite precipitation on different endodontic sealer surfaces in simulated body fluids (Fig. 7f).

Resin based sealer and Zinc oxide non-eugenol sealer didn't revealed apatite precipitation. MTA containing resin-based sealer slightly revealed apatite precipitation. On the other hand, it shows clear needle-like apatite precipitation on PPL containing MTA sealer.

pH measurement of different endodontic sealers

PPL containing MTA sealer was stably holding pH=12, MTA containing resin-base sealer was slightly lower than PPL containing MTA sealer, but it also stable pH=11-12. The pH of Resin based sealer and Zinc oxide non-eugenol sealer was approximately 8-10 (Fig. 7g).

Cell viability

For three endodontic sealers; MTA containing resin based sealer, resin-based sealer and Zinc oxide non eugenol sealer, the higher the dilution of the eluted medium, the higher the cell viability. On the other hand, PPL containing MTA sealer showed the same cell viability as the control group even with the undiluted eluted medium (100%) (Fig. 7h).

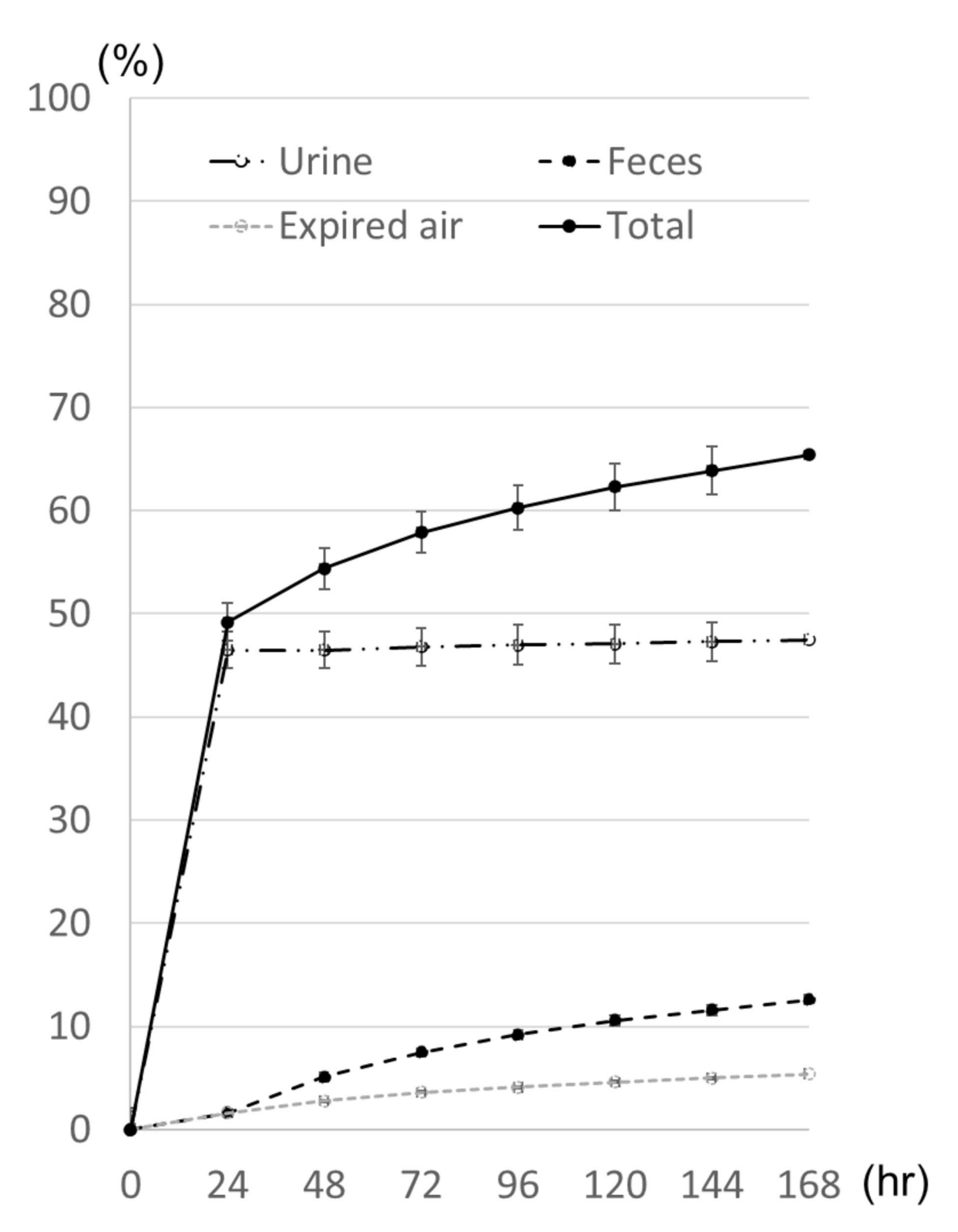


Fig. 6. Pharmacokinetics of 14-C labeled phosphopullulan. Cumulative excretion ratios of radioactivity in urine, feces and expired air following 1% [14C] phosphorylated PPL to rat (mean \pm SD). Measurements of cadavers at 168 h post-dose showed 32.2 \pm 2.4% of the dose in the body.

Discussion

Bioresorbable materials that can be implanted in vivo, integrate into living tissue for a period of time, and are subsequently resorbed are highly valuable for filling hard and soft tissue defects and serving as carriers for drug delivery. Bioabsorbable materials must be endotoxin-free and have assured safety. Consequently, numerous biofilling and drug delivery materials have been studied, but few have reached practical application. In this study,

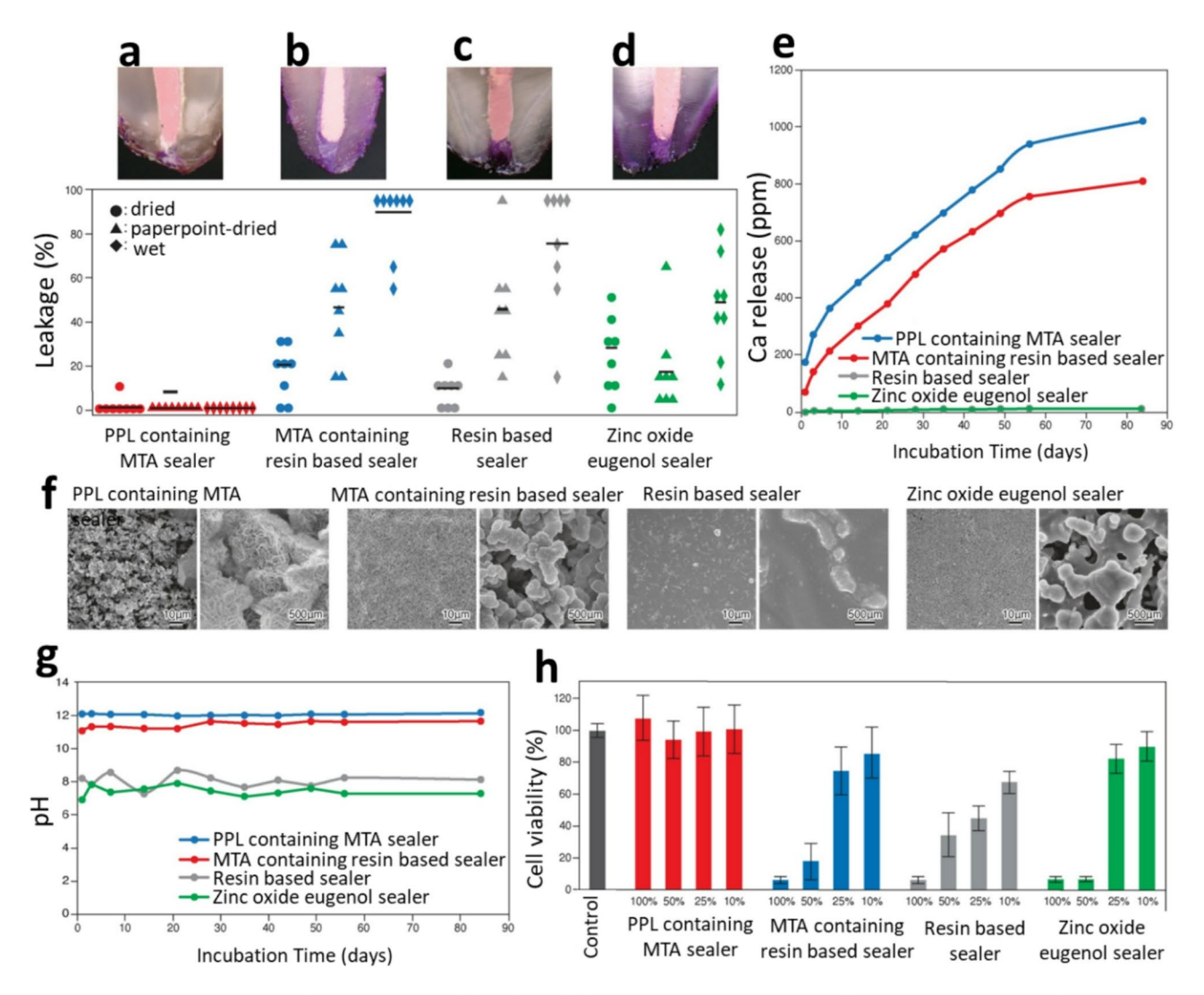


Fig. 7. Characterization of Phosphopullulan (PPL)-containing MTA sealer (\mathbf{a} - \mathbf{d}). Cross section observation of typical dye leakage after root canal treatment with different endodontic sealer. Phosphopullulan (PPL) -containing MTA sealer, resin-based sealer (AH Plus), MTA-containing resin-based sealer (Fillapex), and Zinc oxide non-eugenol sealer (Canals N). Dye leakage (%) of different endodontic sealers with different dentin treatments (paper-point, dry, and wet treatments denoted by a black circle, triangle, and square, respectively). Leakage test revealed that MTA cement with 10% phosphopullulan bonded to dried, paper point dried, and wet dentin surfaces completely prevented interfacial dye infiltration (p<0.01), whereas the MTA cement without phosphopullulan could not prevent die infiltration at all. (\mathbf{e}) Calcium release of different endodontic sealers. \mathbf{f} . Apatite precipitation on different endodontic sealer surface in simulated body fluids. \mathbf{g} . \mathbf{p} H measurement of different endodontic sealers. \mathbf{h} . Cell viability of different endodontic sealers. PPL containing MTA sealer (100%) revealed significantly higher cell viability than compared to the other three commercial sealers (p<0.01).

we report on the endotoxin-free synthesis of phosphopullulan, developed based on bioadhesion theory, as well as its efficacy and safety.

The cross-linking of phosphorylated pullulan molecules is advantageous as they are the key material responsible for adhesion to biological hard tissues (Fig. 1a). Long molecules on a linear chain have more functional groups to bind with substrates, but their viscosity increases and wetting decreases¹⁷ (Fig. 1b,c); therefore, they cannot contribute to adhesion. In contrast, two-dimensional molecules composed of two cross-linked short-linear molecules, inspired by starfish, have more bonding sites for apatitic substrates. They can spread by forming a flat molecule on the substrate surface, resulting in stable adhesion. Phosphopullulan molecules with different molecular weights and characteristics can be synthesized for various uses. Similar to phosphomannan, phosphorylated polysaccharides are generally difficult to dissolve in water. They are highly viscous upon dissolution, making it difficult to produce low-viscosity solutions and films. Phosphopullulan can be obtained in various forms: low-viscosity and high-viscosity solutions, powders, gels, and films (Fig. 1f).

We demonstrated the adhesive capability of the synthesized phosphopullulan using method (3). Materials for tooth and bone restoration should have strong sealing properties to prevent bacterial infections and soft tissue infiltration at sites of leakage^{18,19}. However, the surface of living tissue is typically wet, adversely affecting the adhesion of the restorative materials. Novel functional materials that act as adhesives to wet hard-tissue surfaces are required.

Phosphopullulan with an average molecular weight of 300,000 to 500,000 is used as an additive for root canal filling sealers. According to Japan's National Health Insurance, the annual number of dental root canal filling treatments is > 13 million²⁰, which is more than 10% of Japan's population. The apical root canal cannot be completely moisture-proofed²¹, and even optimized commercial root canal filling sealers cause leakage at the root canal dentin interface. This leads to the reapplication of the sealers. Recently, MTA has been widely used as an endodontic material²² because of its biomineralization and bactericidal properties. However, MTA does not adhere to hard biological tissues. Therefore, it is necessary to improve the sealing properties of the root canal, while maintaining the bactericidal and calcium-release properties of MTA. Leakage test revealed that although MTA cement without phosphopullulan could not prevent interfacial dye infiltration, MTA cement containing only 10% phosphopullulan bonded to dried, paper-point dried, and wet dentin surfaces completely prevented the dye infiltration (Fig. 7a). This finding indicated that MTA cement with 10% phosphopullulan showed the highest sealing ability toward dried as well as wet dentin. This property is not exhibited by any of the currently used dental bonding materials. Moreover, even when 10% phosphopullulan was added to the MTA, its clinically significant characteristics, such as biomineralization and bactericidal abilities, were maintained. MTA is a bioactive material owing to its ability to produce biologically compatible carbonated apatite. The biomineralization ability of the MTA cement containing 10% phosphopullulan was confirmed by the sustained release of Ca (Fig. 7e) and apatite precipitation on its surface in simulated-body fluids (Fig. 7f). MTA cement, which exhibits strong basicity of approximately pH 12, has excellent bactericidal effects. However, some additives may decrease the pH, impairing the sterilization effect. MTA cement containing 10% phosphopullulan is highly bactericidal owing to its stable basicity of approximately pH 12 (Fig. 7g) and high sealing ability (Fig. 7c). Despite the high pH, MTA containing 10% phosphopullulan showed good cell viability in the cytotoxicity test (Fig. 7h), which is necessary for its practical application. Thus, it was confirmed that the MTA cement containing 10% phosphopullulan is effective as a highly functional root canal filling sealer.

Phosphopullulan molecules with a molecular weight exceeding 600,000 form a three-dimensional structure and have the potential to serve as scaffolding/complementary materials for regenerative medicine. Phosphopullulan gels were implanted into bone defects in rabbits (Fig. 5a). The gel was absorbed gradually, and bone formation progressed with time, becoming laminar 9 weeks after implantation (Fig. 5b). Phosphopullulan gels were present within or outside trabecular woven bone and were resorbed by osteoclasts and foreign-body giant cells, respectively, but not by other inflammatory cells Thus, the gel promoted bone formation without any harmful host response, indicating its high biocompatibility and osteoconductivity. Based on these non-clinical studies, a bioadhesive gel containing high-molecular-weight phosphopullulan has been commercialized as a bone regeneration material for cleft lips and palates (Fig. 5c). Treatment of the cleft jaw requires harvesting of the cancellous bone from the healthy iliac bone. Granular artificial bone cannot be used in the cleft jaw because it resorbs slowly in the body and inhibits tooth eruption. To avoid the surgical invasiveness of iliac bone harvesting, a bone replacement material containing phosphopullulan is being developed under the "Strategy of SAKIGAKE²⁶," a system established by the Ministry of Health, Labour and Welfare (MHLW) to support the development of pharmaceuticals and medical devices that are expected to be innovative and effective from basic research to practical application; this system reduces the approval review period by half before practical application. Phosphopullulan can be applied to other bone defect sites as well as other organs and drug delivery

A major problem in non-animal origin polymers is the removal of endotoxins^{27,28}, which cause fever, a temporary decrease in the number of leukocytes, and death when injected in large amounts in the human body. Therefore, removal of endotoxins is indispensable for the practical use of injectable materials. The amount of pullulan²⁹ produced by bacteria during production is highly variable³⁰ (average, 54,000 EU/g). Endotoxin inactivation requires hydrothermal treatment at 250 °C for more than 30 min, which is unsuitable for organic materials. Even with heat treatment at 170 °C in method (1), brownish phosphopullulan was produced via caramelization. The coloration of phosphopullulan interferes with accurate endotoxin measurements, making method (1) an unsuitable production method. Furthermore, heat treatment at 170 °C for 5 h is insufficient for endotoxin inactivation. The amount of endotoxin in the produced phosphopullulan reached 123,520 EU/g, which can be harmful for the body. In method (2), a heterogeneous reaction produced partially caramelized phosphopullulans. The amount of endotoxin was greater than 29,000 EU/g. Highly viscous solutions containing phosphopullulan cannot be used as filters to remove endotoxins and must be adjusted to prepare a dilute solution, leading to increased costs. Moreover, phosphopullulan is a polymer with phosphate groups, and its electrification is similar to that of lipopolysaccharide. This finding indicates that removing the endotoxins from the final product is extremely difficult. Therefore, we considered the inactivation of endotoxins during the process of phosphorylation. The amount of endotoxin in phosphopullulan produced using the phosphoryl chloride method was below detectable limit (<0.78 EU/g). To confirm the bioabsorbability of the synthesized phosphopullulan using method (3), ¹⁴C-labeled phosphopullulan was injected into the abdominal cavity of mice to analyze its behavior in the body. ¹⁴C was detected in the exhaled air, indicating that the high-molecular-weight phosphopullulan was bioresorbable (Fig. 6).

The biocompatibility of phosphopullulan was examined by implantation into rat subcutis (Fig. 5a). The phosphopullulan gels were replaced by normal connective tissues during angiogenesis (Fig. 5b). Phosphopullulan gel was phagocytosed by macrophages with foamy and basophilic cytoplasm; the involvement of other inflammatory cells was minimal (Fig. 3). The macrophages were CD68+/iNOS-/Arg1-, indicating that they

activated phagocytosis but not inflammation and fibrosis (Fig. 5a). Thus, our pyrogen-free phosphopullulan is highly biocompatible and has the potential to remodel normal tissues.

Unlike other organic polymers, phosphopullulan can also be used for gamma sterilization. Cross-linked reticulated polymers are more resistant to gamma rays than linear polymers. Final sterilization by gamma irradiation is a major consideration during the design and manufacture of materials for internal implantation.

Leakage tests have revealed dye infiltration throughout the adhesive interface between MTA cement containing 10% 3,4-dihydroxyphenylalanine (DOPA)^{31,32} and dentin. This cement resulted in detachment of the adhesive interface from the dentin owing to insufficient solidification. One of the crucial functions of additives is to improve the performance of the final composition. Low-molecular-weight phosphopullulan can be used as a component of restorative materials that require flowability, such as root canal filling sealers. The addition of phosphopullulan also improved the operability of MTA cement. Phosphopullulan with an average molecular weight of 300,000–500,000 is used as an additive in root canal filling sealers and has low viscosity when dissolved in water. Therefore, it can be used as a component of restoration materials that require fluidity, such as root canal filling sealers.

Materials and methods Ethics statement

Guidelines adhered to for animal and human sample experiments

Research using human samples is conducted in compliance with the Japanese guidelines for human subjects: Ethical Guidelines for Medical and Health Research Involving Human Subjects and approved by Ethical Review Board for Life Science and Medical Research, Hokkaido University Hospital (project no: 2017-2). Appropriate informed consent was given according to the guidelines.

In addition, all relevant guidelines and regulations, especially the ARRIVE guidelines, have been fully considered and followed in the experiments on vertebrate animals in this study and in the methods used. In addition, experimental procedures have been approved by the respective biomedical research ethics committees for each project. The Ethics Committee approval numbers and the methods of euthanasia performed are listed on each research method.

Phosphopullulan synthesis

Synthesis method 1

The pH of the aqueous solution of pullulan (Hayashibara co. ltd, Okayama, Japan) was adjusted using phosphoric acid and sodium hydroxide, and water was removed by heating at 170 °C for 5 h. The resulting cake-like material was crushed to increase surface area and facilitate removal of water because phosphorylation is an equilibrium reaction, and removal of water is assisted in shifting equilibrium toward phosphate production. The resulting product was dissolved in water, dialyzed, and lyophilized to obtain the product.

Synthesis method 2

A mixed powder of sodium hydrogen phosphate, sodium dihydrogen phosphate, and pullulan was heated using microwave irradiation while stirring (START SYNTH, Milestone Inc., CT, USA).

Synthesis method 3

Pullulan was dissolved in an aqueous sodium hydroxide solution and allowed to incubate overnight. Subsequently, phosphoryl chloride was added, and after the reaction, the remaining phosphoryl chloride was decomposed and neutralized by phosphoric acid. The product was dialyzed (fractional molecular weight 12,000) to remove phosphate and sodium chloride and lyophilized.

Endotoxin measurement

The samples ($200~\mu$ L) were added to tubes containing LAL reagent (Limulus ES-II; FUJIFILM Wako Pure Chemical Corporation, Tokyo, Japan). After mixing the reaction mixture for a few seconds, the test tubes were placed into a ToxinometerET-6000 (FUJIFILM Wako Pure Chemical Corporation, Osaka, Japan) to measure endotoxin activity. The kinetic-turbidimetric assay performed using the toxinometer considered the time required before the appearance of turbidity when a sample containing endotoxin was mixed with the LAL reagent. Endotoxin activity was determined based on the amount of time required for the transmitted light ratio to decrease below a certain threshold (94.9% of the initial value), which is known as the gelation time. Its sensitivity range was 0.0078^{-1} EU/mL. When the endotoxin activity of the sample was higher than 1 EU/mL, the sample was remeasured after dilution using endotoxin-free water (Japanese Pharmacopoeia Reference, Otsuka distilled water, Japan). When the endotoxin activity of the sample had a minimum detection level of 0.0078 EU/mL, it was determined to be below the detection limit. Endotoxin recovery rates of 50 to 200% were considered valid. Endotoxin recovery was equal to the known spike concentration, ranging from 50 to 200%.

Fourier-transform infrared spectroscopy (FTIR)

Freeze-dried phosphopullulan (PPL) and pullulan (PL) samples were prepared and were analyzed using a spectrophotometer (IRAffinity-1 FTIR; Shimadzu, Kyoto, Japan) with a potassium bromide plate (Jasco, Tokyo, Japan) in transmission mode. The spectra of each sample were recorded using 256 scans at a spectral resolution of $4 \, \mathrm{cm}^{-1}$.

¹H NMR and ³¹P NMR measurement

¹H NMR spectra were obtained using a Varian 400MR (Varian, Palo Alto, CA, USA). PL and PPL were dissolved in deuterium oxide (D₂O) at a concentration of 1%. Trimethylsilyl propanoic acid (TMSP, Sigma-Aldrich, St.

Louis, MO, USA) was used as an internal reference for the aqueous solvent, D₂O. The samples were measured 16 times in the 400 MHz frequency band. VNMRJ 3.0 (Varian) was used for data acquisition, and Mnova software (Mestrelab Research, Santiago de Compostela, Spain) was used for data processing.

Titration curve

PPL solution was treated with a column filled with cation exchange resin (Amberlite RB120B H AG, Organo, Tokyo, Japan) to remove the sodium ions attached to the phosphate group. The treated solution was titrated with 0.01 M sodium hydroxide solution.

Reaction of different metal ion

Stress was measured in a Teflon mold with a diameter of 8 mm and a height of 2 mm using 0.20 g of PPL and 150 μ L of aqueous solutions of metal salts of different valence (NaCl, CaCl2, AlCl3) using a universal testing machine.

Alexa Fluor 750-labelled PPL and IVIS imaging

Alexa Fluor 750 (Thermo Fisher Scientific, MA, USA) labelled phosphopullulan was synthesized as follows: hydroxy group of PPL was left to react with allyl bromide to incorporate the allyl group. Then, the amino group was attached to the allyl group by reacting with 2-aminoethanethiol. Alexa Fluor 750 was attached to the amino group.

Animal studies were performed in accordance with the ethical standards of the Committee for Animal Experiments Ethics of Okayama University (approval number: OKU-2012664). The mice were anesthetized and placed on the imaging stage of the IVIS apparatus in the abdominal position. Images were collected at indicated intervals after Alexa Fluor 750 -labeled phosphopullulan subcutaneous implantation using the IVIS Imaging System (Xenogen, Alameda, CA, USA). Photons emitted from the tumor and its surroundings were quantified using Living Image Software (Xenogen). After experiment, under anesthesia with an intraperitoneal injection of ketamine (0.1 mg/g) and xylazine (0.01 mg/g), mice were euthanized by cervical dislocation.

POLARIC labelled PPL and Cell phagocytosis test

POLARIC (Goryo Chemical, Sapporo, Japan) was synthesized as follow: POLARIC-COOH was mixture with phosphopullulan. Then, 4-(4,6-dimethoxy-1,3,5-triazin-2-yl)-4-methylmorpholinium chloride (DMT-MM) was add as dehydration condensation agent at room temperature. After stirring at room temperature, PPL was obtained by freeze drying.

POLARIC-labeled PPL was added to the culture media of the RAW264.7 cells (macrophages) and osteoclasts. Phagocytosis by both cell types was observed with a fluorescence and confocal laser microscope at 2, 12, 24, and 48 h.

To analyze the uptake of phosphorylated pullulan into peritoneal exudate cells, animal study was performed. Animal studies were performed in accordance with the ethical standards of the Committee for Animal Experiments Ethics of Okayama University (approval number: OKU-2012664). Mice received 1 mL of 4% thioglycollate. After 18 h, mice were injected with POLARIC-labeled PPL (0.1 mg/mL, 100 μ L), and 6 h later (24 h after thioglycollate injection), peritoneal lavage fluids were harvested, and the cells were stained with FITC-Gr-1 or F4/80. Cells were observed using fluorescence microscopy and confocal laser microscopy. Under anesthesia with an intraperitoneal injection of ketamine (0.1 mg/g) and xylazine (0.01 mg/g), mice used in the experiment were euthanized by cervical dislocation.

Animal study

Animal studies were performed in accordance with the ethical standards of the Animal Experiments Ethics of Chitose Laboratory, Japan Food Research Laboratories (approval no. HK200703-01). The animals were anesthetized with cocktails of medetomidine, midazolam, and butorphanol (0.4 mg/kg, 4.0 mg/kg, and 4.0 mg/ kg, respectively) via intravenously and subcutaneously³³. The PP620f. gel was implanted into the subcutaneous tissues of JclBrlHan:WIST male rats (CLEA Japan, Tokyo, Japan) at 0.2 g/site for 2 and 4 weeks or into a drilled hole with 4 mm diameter and 8 mm depth in the femurs and tibiae of Japanese White rabbits (Kitayama Labes, Nagano, Japan) at 0.1 g/site for 4 and 9 weeks. After the animals were sacrificed by intravenous injection of sodium pentobarbital, the implanted tissues were fixed with 10% neutral buffered formalin and rabbit bones were decalcified with Morse's solution (20% formic acid and 10% citric acid). The implanted sites were embedded in paraffin and sliced at 4 µm thickness. The subcutaneous and bone sections were stained with hematoxylin and eosin (HE), alcian blue (pH 2.5) and picrosirius red, and JFRL staining³⁴. For immunohistochemistry, deparaffinized sections were heated with 0.01 M sodium citrate buffer (pH 6.0) for 20 min at 105 °C and treated with 0.3% hydrogen peroxidase/ethanol solution for 30 min to eliminate endogenous peroxidase. The slides were incubated with the blocking reagent (Nichirei, Tokyo, Japan) for 30 min, followed by rabbit anti-CD68 polyclonal antibody (ab125212, 1:1000, Abcam, Cambridge, UK), rabbit anti-CD206 monoclonal antibody (clone E6T5J, 1:1000, Cell Signaling, MA, USA), rabbit anti-NOS2 polyclonal antibody (M-19, 1:300, Santa Cruz, CA, USA), or rabbit anti-Arginase-1 monoclonal antibody (clone D4E3M, 1:500, Cell Signaling) overnight at 4 °C. Next, the sections were treated with secondary antibodies (Nichirei) for 30 min, followed by treatment with streptavidinperoxidase (Nichirei) for 30 min. Immunopositive reactions were developed using a 3,3'-diaminobenzidine tetrahydrochloride-H₂O₂ solution. The sections were counterstained with hematoxylin.

Determination of excretion rate in urine, feces, and exhaled air and percentage of residual in the body using ¹⁴C phosphorylated pullulan

Animal studies were performed in accordance with the ethical standards of the Committee for Animal Experiments Ethics of SEKISUI MEDICAL CO., LTD. (Tokyo, Japan) (approval number:2014-105). Male rats (Crl: CD1, 6 weeks old and weighing 200 g at the beginning of the experiments; Charles River Laboratories Japan, Inc., Yokohama, Japan) were used. The rats were intraperitoneally (i.p.) injected with a single dose of 0.5 mL/body of 1% ¹⁴C-phosphorylated pullulan solution. Following the injections, the rats were observed every 24 h for 7 days. The radiation doses of urine, feces, and exhaled breath at each period were examined using a liquid scintillation counter. (HIONIC-FLUOR, PerkinElmer). The rats were sacrificed at 168 h by carbon dioxide inhalation. Post-mortem radiation dose of rats was also examined.

Leakage test using human teeth

A total of 96 non-caries extracted human teeth, with single, straight root canals, but without open apices, were selected. The research protocol was approved by Ethical Review Board for Life Science and Medical Research, Hokkaido University Hospital (project no: 2017-2). The crowns of the teeth were sectioned at 15 mm from the root under water cooling. Working length was visually determined by subtracting 1 mm from the length of 25 K-file at the apical foramen. All canals were instrumented to a working length with a size 40 K-file using the step-back technique. The root canals were irrigated with 1 mL of 5.25% NaOCl while instrumenting them. Patency of the apical foramen was confirmed using size 10-15 K-files. Following root canal preparation, the canals were irrigated with 2 mL of 17% ethylenediaminetetraacetic acid (EDTA) and 10 mL of 10% NaOCl using a syringe with a 23-gauge needle. Finally, the root canals were flushed with 3 mL of distilled water, and the specimen surface was prepared using three different dry protocols as follows: 1) water removal (wet), 2) drying using air-blowing (dry), or 3) drying with sterile paper points (paper-point dry). The prepared teeth were randomly divided into four groups of eight teeth each based on which of the following filling material was used: 1) gutta-percha cones + resin-based sealer (AH plus; Dentsply Sirona, Charlotte, NC, USA), 2) guttapercha cones + zinc oxide-non-eugenol sealer (Canals N; Showa Yakuhin Kano, Tokyo, Japan), 3) gutta-percha cones+PPL-containing MTA sealer, or 4) gutta-percha cones+resin-based sealer MTA fillapex (Angelus, Londrina PR, Brazil). After root canal filling, the root surfaces, except for the apical canal, were covered with nail varnish, and 0.5% basic fuchsin solution was introduced into the root canal through the apical canal at 200 mm H2O using the fluid filtration method after 24 h of storage at 37 °C and 100% humidity. The root was then cut in the axial direction, and dye penetration through the apical foramen was observed using a digital microscope (VHX-5000, Keyence Corporation, Osaka, Japan). Statistical analysis was performed using the Kruskal-Wallis test and Dunnett's test with SPSS Statistics (version 22.0; IBM, Armonk, NY, USA) and a significance level of 5%.

Dye penetration test

The crowns of cryopreserved extracted bovine teeth were excised, the pulp was removed, and six $5 \times 5 \times 1$ mm pieces of dentin were prepared from one root. The surfaces were then ground using #600 waterproof abrasive paper to prepare an adherent surface. The surfaces were treated as follows: treatment with 17% EDTA (17% EDTA Liquid, Pentron Japan Inc., Tokyo, Japan) for 5 min, rinsing with water, air-drying, and 10% NaOCl (Neo Cleaner "Sekine", Neo Pharmaceutical Industries Co.) treatment. EDTA and NaOCl treatments were performed by immersing the dentin pieces in 3 mL of each chemical, and rinsing was performed with 5 mL of distilled water using a syringe. Three different surfaces were prepared—namely wet, dry, and paper-point dry—as described above. Four different seals were prepared and then applied to the adherent surface in approximately 4 mm diameter, and another piece of dentin treated in the same way was placed such that the adherent surface was in contact with the sealer. A second piece of dentin was placed in the same manner and allowed to heal for 24 h at 37 °C and 100% humidity. The specimens (n = 8) were coated with nail varnish, except for the adhered surface, and immersed in 0.5% basic fuchsin solution (Basic Fuchsin, Wako Pure Chemical Industries). Seven days later, the specimens were removed and embedded in epoxy resin (EpoFix/SpeciFix-20; Marumoto Struers Co. Ltd., Tokyo, Japan), and cut in perpendicular direction to the adherent surface at the center of the specimen. The distance of dye penetration into the interface between the sealer and dentin surface was measured using a digital microscope (VHX-5000, Keyence Corporation, Osaka, Japan).

pH measurement

The following four root canal materials were prepared: PPL-containing MTA sealer, resin-based sealer (AH plus), MTA-containing resin-based sealer (MTA fillapex), and zinc oxide non-eugenol sealer (Canals N). Each material was mixed into a hardened body according to the manufacturer's instructions and inserted into an acrylic mold (length, 2 mm; inner diameter, 10 mm). Five samples were used for each experiment. Each sample was stored at 37 °C and 100% humidity for 24 h and soaked in deionized water. pH was measured using a pH meter (D-52, Horiba, Kyoto, Japan) 1 and 3 days and 1, 2, 3, 4, 5, 6, 7, 8, and 12 weeks after soaking³⁵.

Observation using scanning electron microscopy

For each group, ten cylindrical cement blocks of 5 mm diameter and 1 mm thickness were prepared. Each specimen was stored at 37 °C for 24 h at 100% humidity. Half of the blocks were immersed in distilled water, and the other half in simulated body fluid (SBF) for 7 days. The samples were then washed with distilled water and dehydrated using ethanol. Subsequently, a thin layer of osmium was deposited on their surfaces (NeoOsmium coater, Meiwa, Osaka, Japan), and the specimens were then examined using a field emission gun–scanning electron microscope (JSM-6701F, JEOL, Tokyo, Japan) operated at 5 kV with an annular semiconductor detector.

Ca release

Each sample was prepared according to the manufacturer's instructions, and the experimental sealer was mixed with distilled water at a ratio of 3:1 by weight. Samples were sealed in an acrylic ring with an inner diameter of 10 mm and a height of 2 mm and allowed to cure for 24 h at 37 °C and 95% humidity. The samples were immersed in 10 mL of deionized water at 37 °C, rotated in a rotary incubator, and the amount of Ca²⁺ eluted was measured after 1 and 3 days and 1 and 2 weeks using inductively coupled plasma-optical emission spectrometry (iCAP 7200 ICP, Thermo Fisher Scientific, Kanagawa, Japan)³⁵.

Cytotoxity

For cytotoxicity tests, a test protocol strictly according to the ISO 10993-5 standard was followed^{35–37}. Silicone molds with a diameter of 10 mm and a height of 1.5 mm (approximately 2.0 cm²) were filled with the root canal sealer. For the light-curable resin-based MTA sealer, Fillapex was light-cured for 20 s from both sides using a light curing device (G-light plima, GC). Nine specimens were prepared for each experimental group. All specimens were kept at saturated humidity in a 37 °C incubator for 24 h, prior to being immersed in 650 mL of extraction Dulbecco's minimum essential medium (DMEM; Sigma-Aldrich) with 5% fetal bovine serum (FBS) and 1% penicillin-streptomycin for 24 h in a 37 °C incubator, after which the extracts were collected. The extracts were filtered using a 0.20 mm filter. Chinese hamster fibroblasts (V79-4, ATCC CCL-93) were routinely cultivated in DMEM with 5% FBS and 1% penicillin-streptomycin at 37 °C with 5% CO2. In the medium, 100 mL cells were seeded in 96-well plates at 5×10³ cells per well and incubated for 24 h at 37 °C. The medium was then replaced by medium containing undiluted or 50% diluted cement extract. For each group, cells were seeded into three wells. After 24 h incubation at 37 °C, the medium was removed, and cell survival was determined using an MTT assay (Sigma-Aldrich). After adding 10 mL of MTT solution to each well, the cells were incubated for an additional 4 h. The resulting formazan crystals were dissolved by replacing the culture medium in each well with 90 mL dimethyl sulfoxide (Sigma-Aldrich). After storing the plates overnight, the absorbance at 450 nm was determined using a microplate reader (Multiskan Ascent 96/384; Thermo Electron, Waltham, MA, USA). The results were presented as the percentage of cell viability with respect to those incubated without materials (control). This procedure was repeated thrice. Statistical analysis was performed using two-way ANOVA and Tukey's HSD test at a significance level of a = 0.05 using IBM SPSS Statistics (version 22; IBM).

Data availability

The data that support the findings of this study are available from the corresponding author, upon reasonable request.

Received: 15 December 2024; Accepted: 17 April 2025

Published online: 12 June 2025

References

- 1. Park, S. B., Lih, E., Park, K. S., Joung, Y. K. & Han, D. K. Biopolymer-based functional composites for medical applications. *Prog. Polym. Sci.* 68, 77–105 (2017).
- Kalidas, V. K., Pavendhan, R., Sudhakar, K., Sumanth, T. P. & Kumar, K. Y. Study of synthesis and analysis of bio-inspired polymers-review. *Mater. Today Proc.* 44, 3856–3860. https://doi.org/10.1016/j.matpr.2020.12.831 (2021).
- 3. Asadi, N., del Bakhshayesh, A. R., Davaran, S. & Akbarzadeh, A. Common biocompatible polymeric materials for tissue engineering and regenerative medicine. *Mater. Chem. Phys.* 242, 122528. https://doi.org/10.1016/j.matchemphys.2019.122528. (2020).
- Schneier, M., Razdan, S., Miller, A. M., Briceno, M. E. & Barua, S. Current technologies to endotoxin detection and removal for biopharmaceutical purification. *Biotechnol. Bioeng.* 117, 2588–2609. https://doi.org/10.1002/bit.27362 (2020).
- Pereira, S. B. et al. Strategies to obtain designer polymers based on cyanobacterial extracellular polymeric substances (EPS). Int. J. Mol. Sci. 20, 5693. https://doi.org/10.3390/ijms20225693 (2019).
- 6. Parodi, A. The potential of future foods for sustainable and healty diets.. *Nat. Sustain.* 1, 782–789. https://doi.org/10.1038/s41893-0 18-0189-7. (2018).
- Zhang, L., Liu, M., Zhang, Y. & Pei, R. Recent progress of highly adhesive hydrogels as wound dressing. Biomacromol 21, 3966–3983. https://doi.org/10.1021/acs.biomac.0c01069 (2020).
- 8. Ahadian, S. et al. Organ-On-A-chip platforms: A convergence of advanced materials, cells, and microscale technologies.. *Adv. Helthec. Mater.* 7, 1700506. https://doi.org/10.1002/adhm.201700506 (2018).
- Xue, X., Hu, Y., Deng, Y. & Su, J. Recent advances in design of functional biocompatible hydrogels for bone tissue engineering. Adv. Funct. Mater. 31, 2009432. https://doi.org/10.1002/adfm.202009432 (2021).
- 10. Armiento, A. R., Hatt, L. P., Sanchez Rosenberg, G., Thompson, K. & Stoddart, M. J. Functional biomaterials for bone regeneration: Alesson in complex biology. *Adv. Funct. Mater.* **30**, 1909874 (2020).
- 11. Okuchi, J. et al. Wnt-modified materials mediate asymmetric stem cell division to direct human osteogenic tissue formation for bone repair. Nat. Mater. 20, 108–118 (2021).
- 12. DeRocher, K. A. et al. Chemical gradients in human enamel crystallites. *Nature* 583, 66-71 (2020).
- 13. Yoshida, Y. et al. Comparative study on adhesive performance of functional monomers. J. Dent. Res. 83, 454–458. https://doi.org/10.1177/154405910408300604 (2004).
- Ghanadpour, M., Carosio, F., Larsson, P. T. & Wågberg, W. L. Phosphorylated cellulose nanofibrils: A Renewable nanomaterial for the preparation of intrinsically flame-retardant materials. *Biomacromol.* 16, 3399–3410. https://doi.org/10.1021/acs.biomac.5b011 17 (2015).
- 15. Takahata, T. et al. Bone engineering by phosphorylated-pullulan and β -TCP composite. *Biomed. Mater.* 10, 065009. https://doi.org/10.1088/1748-6041/10/6/065009 (2015).
- Ablouh, E. H. et al. A highly efficient chemical approach to producing green phosphorylated cellulosic macromolecules. RSC Adv. 11, 24206–24216. https://doi.org/10.1039/d1ra02713a (2021).
- 17. Mizuno, H. L. et al. Relationship between bulk physicochemical properties and surface wettability of hydrogels with homogeneous network structure. *Langmuir* 36, 5554–5562 (2020).
- 18. Baras, B. H. et al. Novel bioactive root canal sealer with antibiofilm and remineralization properties. *J. Dent.* 83, 67–76. https://doi.org/10.1016/j.jdent.2019.02.006 (2019).

- 19. de Avila, E. D., van Oirschot, B. A. & van den Beucken, J. J. J. P. Biomaterial-based possibilities for managing periimplantitis. *J. Periodont. Res.* 55, 165–173. https://doi.org/10.1111/jre.12707 (2020).
- 20. The Ministry of Health, Labor and Welfare. Statistics by Social Medical Practice.
- 21. Nagas, E. et al. Dentin moisture conditions affect the adhesion of root canal sealers. *J. Endod.* 38, 240–244. https://doi.org/10.1016/j.joen.2011.09.027 (2012).
- Tanomaru-Filho, M., Chaves Faleiros, F. B., Saçaki, J. N., Hungaro Duarte, M. A. & Guerreiro-Tanomaru, J. M. Evaluation of pH andcalcium ion release of root-end filling materials containing calcium hydroxide or mineral trioxide aggregate. J. Endod. 35, 1418–1421. https://doi.org/10.1016/j.joen.2009.07.009 (2009).
- 23. Massi, S. et al. PH, calcium ion release, and setting time of an experimental mineral trioxide aggregate-based root canal sealer. *J. Endod.* 37, 844–846. https://doi.org/10.1016/j.joen.2011.02.033 (2011).
- 24. Bogen, G. & Kuttler, S. Mineral trioxide aggregate obturation: A review and case series. *J. Endod.* 35, 777–790. https://doi.org/10.1016/j.joen.2009.03.006 (2009).
- 25. Torabinejad, M. & Parirokh, M. Mineral trioxide aggregate: A comprehensive literature review-part II: Leakage and biocompatibility investigations. *J. Endod.* 36, 190–202. https://doi.org/10.1016/j.joen.2009.09.010 (2010).
- The Ministry of Health, Labour and Welfare of Japan. Strategy of SAKIGAKE. https://www.mhlw.go.jp/english/policy/healthmedical/pharmaceuticals/140729-01.html (2014).
- 27. Koller, M. Biodegradable and biocompatible polyhydroxy-alkanoates (PHA): Auspicious microbial macromolecules for pharmaceutical and therapeutic applications. *Molecules* 23, 362 (2018).
- 28. Debabov, V. G. & Bogush, V. G. Recombinant spidroins as the basis for new materials. ACS Biomater. Sci. Eng. 6, 3745–3761. https://doi.org/10.1021/acsbiomaterials.0c00109 (2020).
- Tabasum, S. et al. A review on versatile applications of blends and composites of pullulan with natural and synthetic polymers. *Int. J. Biol. Macromol.* 120, 603–632. https://doi.org/10.1016/j.ijbiomac.2018.07.154 (2018).
- 30. Shahriari-Khalaji, M. et al. Functionalization of Aminoalkylsilane-grafted bacterial nanocellulose with ZnO-NPs-doped pullulan electrospun nanofibers for multifunctional wound dressing. ACS Biomater. Sci. Eng. 7, 3933–3946. https://doi.org/10.1021/acsbiomaterials.1c00444 (2021).
- 31. Tu, M. G. et al. Mineral trioxide aggregate with mussel-inspired surface nanolayers for stimulating odontogenic differentiation of dental pulp cells. *J. Endod.* 44, 963–970. https://doi.org/10.1016/j.joen.2018.02.018 (2018).
- 32. Lee, H., Scherer, N. F. & Messersmith, P. B. Single-molecule mechanics of mussel adhesion. *Proc. Natl Acad. Sci. U. S. A.* 103, 12999–13003. https://doi.org/10.1073/pnas.0605552103 (2006).
- 33. Iwanaga, R. et al. Dual-route administration of balanced anesthesia using medetomidine, midazolam, and butorphanol provides both suitable anesthetic depth and reduced tissue injury in rabbits. *Exp. Anim.* Advance online publication. https://doi.org/10.153 8/expanim.24-0132 (2024).
- 34. Nakamura, T. et al. Novel polychrome staining distinguishing osteochondral tissue and bone cells in decalcified paraffin sections. *Cell Tissue Res.* 385, 727–737. https://doi.org/10.1007/s00441-021-03516-6 (2021).
- 35. Yoshihara, K. et al. Development of self-adhesive pulp-capping agents containing a novel hydrophilic and highly polymerizable acrylamide monomer. *J. Mater. Chem. B.* **8**, 5320–5329. https://doi.org/10.1039/d0tb00079e (2020).
- 36. International Organization for Standardization. ISO 10993–5:2009. Biological Evaluation of Medical Devices—Part 5: Tests for In Vitro cytotoxicity (2009).
- 37. International Organization for Standardization. ISO 10993–12:2012. Biological Evaluation of Medical Devices—Part 12: Sample Preparation and Reference Materials (2009).

Acknowledgements

This study was supported by governmental funding as following: Japan Agency for Medical Research and Development (AMED) grants JP18hk0102055h0001, JP22hk0102087h0001, and JP22hma322005 and JSPS KAKEN-HI grant 20K09950, 23K18597.

Author contributions

Conceptualization: YY, TO, TS; Methodology: RO, KY, TM, AM, YY; Investigation: RO, KY, TO, MN, TS; Visualization: KN, TA, TP, IT; Funding acquisition: IT, YY; Project administration: YY, TN, TS; Supervision: SS, AM, BVM, YY; Writing – original draft: RO, YY, KY, KN, TA, TN; Writing – review & editing: SS, TO, MN, AM, IT, BAM; All authors approved the final version of the manuscript to be published.

Declarations

Competing interests

The authors declare no competing interests.

Additional information

Correspondence and requests for materials should be addressed to K.Y. or Y.Y.

Reprints and permissions information is available at www.nature.com/reprints.

Publisher's note Springer Nature remains neutral with regard to jurisdictional claims in published maps and institutional affiliations.

Open Access This article is licensed under a Creative Commons Attribution-NonCommercial-NoDerivatives 4.0 International License, which permits any non-commercial use, sharing, distribution and reproduction in any medium or format, as long as you give appropriate credit to the original author(s) and the source, provide a link to the Creative Commons licence, and indicate if you modified the licensed material. You do not have permission under this licence to share adapted material derived from this article or parts of it. The images or other third party material in this article are included in the article's Creative Commons licence, unless indicated otherwise in a credit line to the material. If material is not included in the article's Creative Commons licence and your intended use is not permitted by statutory regulation or exceeds the permitted use, you will need to obtain permission directly from the copyright holder. To view a copy of this licence, visit https://creativecommons.org/licenses/by-nc-nd/4.0/.

© The Author(s) 2025